Neutron diffraction study of the structure and low-temperature phase transformation in ternary NiAl + M (M = Ni, Fe, Co) alloys

L. Yang,[a,b] X.-L. Wang,[a,*] C.T. Liu,[a,c] J.A. Fernandez-Baca,[a] C.L. Fu,[a] J.W. Richardson[d] and D. Shi[b]

[a]Oak Ridge National Laboratory, Oak Ridge, TN 37831, USA
[b]Department of Chemical and Materials Engineering, University of Cincinnati, Cincinnati, OH 45221-0012, USA
[c]Department of Materials Science and Engineering, University of Tennessee, Knoxville, TN 37996, USA
[d]Intense Pulsed Neutron Source, Argonne National Laboratory, Argonne, IL 60439, USA

Neutron diffraction was used to study the structure of ternary NiAl + M (M = Ni, Fe, Co) alloys. The experiment confirmed the predictions by first-principle calculations on site preference by solute atoms. Moreover, a universal structural transformation was observed below 20 K in alloys where Al is partially replaced by M. The extra peaks at low-temperatures do not match those from known martensite phases, but are well indexed by a cubic structure. A possible mechanism for the low-temperature phase is discussed.
© 2007 Acta Materialia Inc. Published by Elsevier Ltd. All rights reserved.

Keywords: Nickel aluminides; Crystal structure; Neutron diffraction; Magnetic structure ordering

Nickel aluminides are intermetallic compounds that exhibit a rich variety of physical phenomena. Despite years of extensive studies, new discoveries are still being made which continue to draw attention to this alloy system. Recently, unusual softening behaviors were reported in a systematic study of ternary $Ni_{60-x}Al_{40}M_x$ alloys, where M is a transition metal atom [1,2]. Significant softening (by as much as 30%) was observed when M = Fe, Cr or Mn, but not so when M = Co. The hardening behavior of random substitutional solid solutions has traditionally been correlated with mismatch in atomic size or elastic moduli, and/or the difference in valence electrons between solute and solvent atoms [1,3]. Here, however, Fe and Co atoms show completely different influence on the hardening behavior of $Ni_{60-x}Al_{40}M_x$ alloys, despite having almost identical Goldschmidt radii. First-principle calculations [1,2] revealed that quantum effects involving magnetic interactions play a key role. In the case of Fe, the inclusion of magnetic interaction leads to spin polarization, which produces a large localized magnetic moment on Fe

atoms. A structural consequence of spin polarization is the substantial increase of the effective atomic size for Fe. As a result, the alloy softens. The increase of the effective atomic size is accompanied by a lattice dilation, which has been observed experimentally. Due to the magnetic interaction, Fe atoms prefer the Al site. For Co-containing $Ni_{60}Al_{40}$ alloys, no softening was observed, and the first-principle calculations predict that Co atoms essentially occupy the Ni site and have no magnetic moment. These combined experimental and theoretical studies suggest a new principle in the design of strong and tough intermetallic and metallic alloys.

To verify the predictions of first-principle calculations, we have carried out a systematic study on the structure and magnetic properties of NiAl + M alloys. The results of the magnetic study have been reported elsewhere by Liu et al. [4]. In particular, the presence of a large magnetic moment on a Fe-containing alloy is confirmed. The structural study was conducted using neutron diffraction. Due to the difference in neutron scattering lengths, which are summarized in Table 1 for the atoms comprising the NiAlM alloys, neutron diffraction is well suited for determining the site preference or occupancy for solute atoms. This is to be contrasted with X-ray diffraction, where the scattering length

---

* Corresponding author. Tel.: +1 865 574 9164; fax: +1 865 574 6080; e-mail: wangxl@ornl.gov

Table 1. Coherent neutron scattering length, b, for constituent atoms comprising the NiAlM solid solution alloys

Atom	Ni	Co	Fe	Al
b (10^{-12} cm)	10.3	2.5	9.5	3.4

contrast for neighboring transition metal atoms is very small. Low-temperature neutron diffraction measurements were also carried out to investigate possible structure transitions below room temperature. The results of the structural study for $Ni_{60-x}Al_{40}M_x$ alloys, with M = Ni, Fe, Co, are presented below.

A summary of the samples used in the neutron diffraction experiment is given in Table 2. $Ni_{60-x}Al_{40}M_x$ alloys were prepared from high-purity elements by arc-melting, then homogenized at 1300 °C for 10 h. As a reference, a $Ni_{41}Al_{50}Fe_9$ alloy (alloy 24), with Fe replacing Ni, was also prepared. Powder samples for neutron diffraction studies were obtained by crushing the brittle ingot with a steel mortar and pestle, then sealed in evacuated quartz capsules and annealed at 950 °C for 1 day. Characterizations of the chemical composition and powder sizes have been detailed by Pike et al. [5,6]. Except for alloy 7, only fine-powder samples with a mesh size of −200 were used for the neutron diffraction experiments. For alloy 7, both fine- and coarse-powder (−40 + 80 mesh size) samples were measured.

Neutron diffraction experiments were conducted at the Intense Pulsed Neutron Source of Argonne National Laboratory, using a general-purpose powder diffractometer. Each type of powder sample was loaded into a vanadium can in a helium glove box, which was then mounted onto the cold finger of a Displex cryostat. For each sample, diffraction patterns were collected for 1–3 h at select temperatures between room temperature and 10 K, both during cool-down and warm-up. The neutron diffraction data were analyzed by Rietveld refinement using the GSAS package [7].

For all samples, the room temperature neutron diffraction patterns are characteristic of a B2 (CsCl) type structure, in which Ni and Al atoms occupy the $(0, 0, 0)$ and body center $(0.5, 0.5, 0.5)$ sites, respectively. Figure 1 is a representative diffraction pattern along with the results of refinement based on the B2 structure. The diffraction peaks for some of the samples (e.g. alloy 7) are broader than the instrument resolution. This is mostly likely due to the substitution of the solute atoms, since annealing at 950 °C for 1 day is expected to eliminate the deformation strains induced by crushing the ingot. In any case, the broadening of the diffraction peaks has been taken into account by allowing the peak-shape
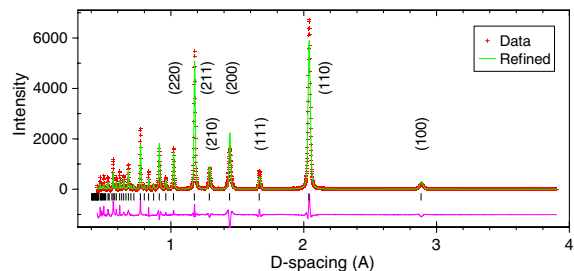
Figure 1. Neutron diffraction pattern of alloy 7 ($Ni_{51}Al_{40}Fe_9$) at room temperature. The crosses are experimental data whereas the solid line through the crosses is a fit based on the ordered body-centered cubic (bcc) (B2) structure. The difference between the experimental data and fit is plotted at the bottom. The tick marks indicate calculated peak positions with the B2 structure.

parameters to vary during the refinement. The refined lattice parameters are shown in Table 2. Indeed, compared with the parent alloy of $Ni_{60}Al_{40}$, the addition of Fe significantly increases the lattice parameter, while the addition of Co produces little change.

Full pattern refinement proceeded first by assuming all solute atoms occupying the Al site. Then, the solute atoms were allowed to choose either Ni or Al sites, while keeping the thermal parameters fixed. After this step, the thermal parameters were released to determine the final site occupancies. The refinement results for select alloys can be found in Table 3 posted on-line.

For alloy 4 ($Ni_{51}Al_{40}Co_9$), the weighted profile R factor (wR_p), a measure of the quality of the refinement, decreased sharply from 8.65% to 7.75% when Co was allowed to move from Al site to Ni site, with more than half of Co settling on Ni site. The isotropic thermal parameter for atoms on the Al site also became more realistic. As shown in Table 1, the neutron scattering lengths for Ni and Fe atoms are quite close, which makes the determination of Fe population difficult. Nonetheless, the refinement showed that for alloy 7 ($Ni_{51}Al_{40}Fe_9$), wR_p increased from 7.51% to 7.89% when Fe atoms were assumed to fully occupy Ni rather than Al site. Moreover, refinement of the site occupancy for Fe at Ni site resulted in negative site occupancy, while wR_p decreased only slightly from 7.51% to 7.47%. These results led us to conclude that in Fe-containing $Ni_{60-x}Al_{40}M_x$ alloys, Fe atoms favor the Al site.

Upon cooling from room temperature, a universal phase transition was observed for all $Ni_{60-x}Al_{40}M_x$ samples. As an example, Figure 2a shows diffraction patterns for alloy 7 (fine-powder sample) at select temperatures from 25 K down to 10 K and back up to 50 K. An extra

Table 2. Composition and nominal site occupancy of samples studied in present neutron diffraction experiment

Sample name	Composition (at.%)	Lattice parameter (Å)	Site preference of solute atoms	Effective magnetic moment (μ_B atom^{-1})
Alloy 1	$Ni_{60}Al_{40}$	2.8664	Al	0.04
Alloy 4	$Ni_{51}Al_{40}Co_9$	2.8657	Ni	–
Alloy 6	$Ni_{55}Al_{40}Fe_5$	*	Al	–
Alloy 7	$Ni_{51}Al_{40}Fe_9$	2.8805	Al	1.8
Alloy 24	$Ni_{41}Al_{50}Fe_9$	2.8875	Ni	0.41

The lattice parameters were obtained from refinement of the room temperature data sets. The effective magnetic moments determined from DC magnetic susceptibility are also listed for select alloys.
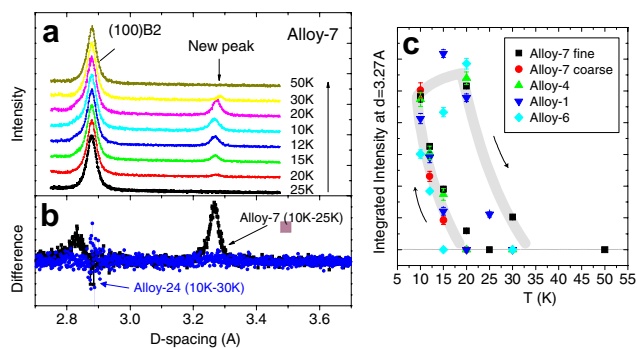*Only low-temperature measurements below 50 K were made.

Figure 2. (a) Diffraction patterns of alloy 7 ($Ni_{51}Al_{40}Fe_9$, fine-powder sample) from 25 K down to 10 K then up to 50 K; (b) difference curves for alloys and alloy 24 ($Ni_{41}Al_{50}Fe_9$). Note that in alloy 7, Fe atoms preferentially occupy Al site, whereas in alloy 24, Fe atoms occupy Ni site. (c) Integrated intensity of the extra peak at $d = 3.27$ Å for all sample under study (normalized to 100 at ∼10 K). For alloy 7, both fine- and coarse-powder samples were measured, as indicated in the legend. The shaded band is a guide to the eye to illustrate the thermal hysteresis of the transition.

peak at $d \sim 3.27$ Å appeared at and below 20 K. Another extra peak, at $d \sim 2.83$ Å, can also be readily identified by subtracting the 25 K data set from the lower temperature data, as illustrated in Figure 2b. Inspection of data from low-angle detector banks, which cover a larger range of the lattice spacing, revealed no additional peaks beyond 3.27 Å. In Figure 2c, the intensity of the extra peak at $d \sim 3.27$ Å was normalized to 100 at 10 K and plotted as a function of temperature. For alloy 7, both fine- and coarse-powder samples were included. Within the precision of the experiment, the data for all $Ni_{60-x}Al_{40}M_x$ alloys overlap with each other and follow a universal trend. A thermal hysteresis is clearly noted; the reverse transition occurred only when the temperature was raised to ∼30 K during warm-up.

No extra peaks were observed when the body-center site is fully occupied by Al. This is demonstrated with alloy 24 ($Ni_{41}Al_{50}Fe_9$), where the solute atoms (Fe) occupy the Ni site. As can be seen from Figure 2b, the diffraction patterns collected at 10 and 30 K are virtually identical.

Refinement of the neutron diffraction data confirms that, for $Ni_{60-x}Al_{40}M_x$ (M = Ni, Fe, Co) alloys, site occupancy indeed depends on solute type. Fe atoms prefer the Al site, while Co atoms slightly prefer the Ni site. The neutron diffraction result for the Fe-containing alloy 7 is also consistent with atom locations determined by channeling enhanced microanalysis (ALCHEMI) reported previously [6].

First-principle calculations provided insights into the site preference of various solute atoms [2]. When a solute atom is incorporated into NiAl, there are two possible configurations: the Ni or the Al site. First-principle calculations predict that the Co atoms take the Ni site preferentially by an energy difference of 0.3 eV per Co atom, due to the similar size of the Ni and Co atoms. Our refinement results show Co populations on both sites, with a slight preference for the Ni site. For Fe solutes, spin-polarization effectively enlarged the Fe atoms, whose atom size approaches that of Al. As a result, the Fe atoms prefer the Al site by 0.1 eV per Fe atom.

Since the energy difference between the two configurations is quite small, it is also quite possible that a small fraction of the Fe atoms occupy the Ni site due to thermal fluctuations; this has been observed experimentally by ALCHEMI analysis [6].

Our neutron diffraction data on alloy 24 ($Ni_{41}Al_{50}Fe_9$) demonstrate that, so long as Al is stoichiometric, the B2 structure is stable down to 10 K. However, a phase transition occurs below $T = 20$ K, when Al atoms are partially replaced by transition metal solute atoms. This is seen universally in all four of the $Ni_{60-x}Al_{40}M_x$ (M = Ni, Fe, Co) alloys that were measured, regardless of the types or amounts of solute atoms.

To determine whether the observed phase transition is due to ordering of magnetic moments, we have also listed in Table 2 the effective magnetic moments for select alloys from susceptibility measurements [4]. The data show that, amongst the alloys investigated, only alloy 7, with M = Fe, develops a large localized magnetic moment. Alloy 1, with M = Ni, for example, exhibits an effective magnetic moment of $0.04\mu_B$, some two orders of magnitude smaller than that of alloy 7. In fact, the magnetic susceptibility for alloy 1 is well characterized by Curie–Weiss behavior throughout the measurement temperature range, with no kinks or indications of a magnetic phase transition from room temperature down to 5 K [4]. First-principle calculations also predicted that neither alloy 1 nor alloy 4, with M = Co, has a magnetic moment. From these considerations, it is clear that the universal phase transition observed in $Ni_{60-x}Al_{40}M_x$ alloys is structural, rather than due to ordering of magnetic moments.

It is natural to consider whether the extra peaks at low-temperature arose from a martensitic transformation, which is known to occur for Ni-rich NiAl alloys [8–10]. There are many variants of the low-temperature martensite phase, depending on the type and composition of solute atoms. Typically, the martensite structure is formed by a stack of $\{1\,1\,0\}$ planes sliding along the $\langle 1 -1\,0\rangle$ directions. In addition, there are also a homogeneous lattice deformation (known as Bain distortion) and a modulation (frequently called shuffles) of the stacking planes. The $L1_0$ phase, with a face-centered tetragonal structure, is a simple form of martensite. In Figure 3a, a low-temperature diffraction pattern for alloy 7 is compared with calculations based on the $L1_0$ phase proposed for $Ni_{63-x}Al_{37+x}$ [11], with $a = b = 3.820$ and $c = 3.265$ Å. Clearly, the calculated peak positions do not match the experimental observations. Other martensite phases have less symmetry and would have produced even more peaks. Thus, it is unlikely that the observed low-temperature phase belongs to any of the known martensite phases. Indeed, from the phase diagram summarized in Ref. [11], $Ni_{60}Al_{40}$ may not exhibit a martensitic transformation at all, as a linear extrapolation of the transition temperature would be below 0 K for this alloy.

Surprisingly, we found that the extra peaks at low temperature can be indexed by a cubic cell, as is shown by the first row of tick marks in Figure 3b. In addition to the main extra peaks at $d \sim 2.83$ and ∼3.27 Å, the small peaks (e.g. at $d \sim 1.52$, 1.57 and 1.71 Å) are also accounted for. The lattice parameter of this cubic phase is 5.655 Å, just under (by about 1.6%) twice that of the B2 cell (at 15 K). A higher symmetry variant of
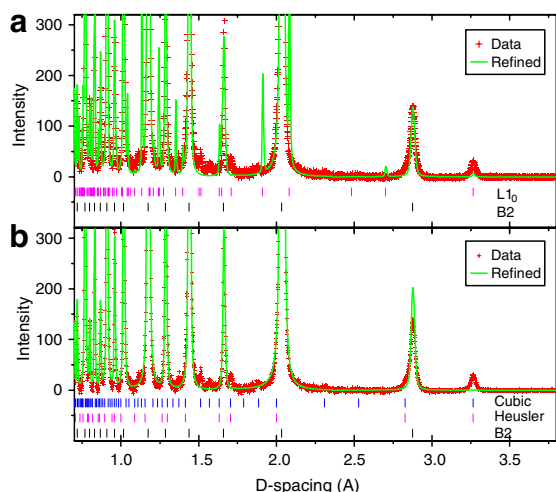
Figure 3. (a) Refinement of the 10 K diffraction pattern for alloy 7 ($Ni_{51}Al_{40}Fe_9$) with two phases: B2 and a small amount of L1$_0$ [11]. (b) Calculated peak positions from a simple cubic structure (the first row) and a Heusler structure (the second row). The lattice parameter is $a = 5.655$ Å for both cases. For comparison, the best refinement results with a B2 structure are also shown to emphasize the appearance of extra peaks throughout the *d*-spacing range.

the proposed cubic phase is the Heusler structure, as shown in Figure 4, with alternating Al and M (Co, Fe, Ni) layers along the [1 1 1] direction. Indeed, the Heusler structure can account for some of the extra peaks (the second row tick marks in Fig. 3b), but miss others due to the face-centered cubic (fcc) symmetry. We also checked the DO$_3$ type of structure, which has fcc symmetry and gives the same number of peaks as the Heusler structure.

Due to the weak intensities of the low-temperature phase, a detailed structure model could not be established at this time. Nonetheless, the good match of peak positions show that a cubic phase with symmetry somewhere between the highly ordered Heusler and the disordered B2 (Al site partially occupied by random substitution of M) is responsible for the extra peaks. The weak intensities associated with the extra peaks also indicate that the transformation is partial and only a small fraction of the material transformed.

The mechanism for this low-temperature phase is still not clear. However, nanoscale composition fluctuation
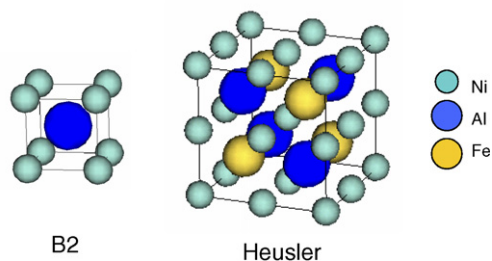

Figure 4. Comparison of B2 and a hypothetical Heusler structure for $Ni_{51}Al_{40}Fe_9$. The low-temperature phase is well indexed by a cubic lattice with a cell parameter slightly smaller than twice that of the B2 structure. Symmetry of the new phase falls between the highly ordered Heusler and the disordered B2 structure, where the Al site is partially occupied by random substitution of Fe.

has been observed in NiAl alloys with similar compositions. Transmission electron microscopy (TEM) results [11] showed that small coherent solute-rich clusters form within the B2 matrix. It is quite possible that the new phase observed in our experiment is related to these solute-rich clusters. From the present experiment, the low-temperature cubic phase formed apparently by ordering of the Al site. Since the B2 to Heusler phase transformation may involve only the movement of the nearest neighbor atoms, it is possible for the transformation to take place even at the low temperature of 20 K. Also, because of the low-temperature transformation, the particle size should be very small. Further experiments, e.g. by TEM or small angle scattering, are needed to clarify the origin of the new phase.

In conclusion, our neutron diffraction study shows the following:

1. In $Ni_{60-x}Al_{40}M_x$ alloys, the solute atoms M show different site preferences. In particular, Fe atoms favors Al site, while Co atoms prefers the Ni site. These observations confirm the prediction by first-principle calculations.
2. A universal structural transformation was observed below 20 K when the Al site is partially replaced by transition metal solute atoms. The new structure appears to be cubic, with symmetry between disordered bcc and fcc.
3. No transformation was observed for alloys with stoichiometric Al.

[1] C.T. Liu, C.L. Fu, L.M. Pike, D.S. Easton, Acta Mater. 50 (2002) 3205–3212.
[2] C.L. Fu, C.T. Liu, X.-L. Wang, M. Krcmar, J.A. Fernandez-baca, Intermetallics 12 (2004) 911–919.
[3] P. Haasen, Mechanical properties of solid solutions and intermetallic compounds, in: R.W. Cahn, P. Haasen (Eds.), Physical Metallurgy, third ed., North-Holland Physics Publishing, New York, 1983, pp. 1341–1408.
[4] C.T. Liu, C.L. Fu, M.F. Chrisholm, J.R. Thompson X.-L. Wang, Prog. Mat. Sci. 52 (2007) 352–370.
[5] L.M. Pike, Y.A. Chang, C.T. Liu, Intermetallics 5 (1997) 601–608.
[6] L.M. Pike, I.M. Anderson, C.T. Liu, Y.A. Chang, Acta Mater. 50 (2002) 3859–3897.
[7] A.C. Larson, R.B. von Dreele, LAUR 86-748 Report 1986; Los Alamos National Laboratory, Los Alamos, NM.
[8] S. Chakravorty, C.M. Wayman, Metall. Trans. 7 (1976) 555–568.
[9] S. Chakravorty, C.M. Wayman, Metall. Trans. 7 (1976) 569–582.
[10] S.M. Shapiro, B.X. Yang, Y. Noda, L.E. Tanner, D. Schryvers, Phys. Rev. B (1991) 9301–9313.
[11] P.L. Potapov, P. Ochin, J. Pons, D. Schryvers, Acta Mater. (2000) 3833–3845.